Journal of Innovative Optical Health Sciences
Vol. 2, No. 1 (2009) 37–43

World Scientific
www.worldscientific.com

COHERENT ANTI-STOKES RAMAN SCATTERING MICROSCOPY TO MONITOR DRUG DISSOLUTION IN DIFFERENT ORAL PHARMACEUTICAL TABLETS

M. JURNA*, M. WINDBERGS†,§, C. J. STRACHAN§,¶,
L. HARTSUIKER‡, C. OTTO‡, P. KLEINEBUDDE†,
J. L. HEREK*, and H. L. OFFERHAUS*

*Optical Sciences Group
MESA+ Institute for Nanotechnology
University of Twente, The Netherlands

†Institute of Pharmaceutics and Biopharmaceutics
Heinrich-Heine University of Düsseldorf, Germany

‡BioPhysical Engineering Group
MESA+ Institute for Nanotechnology
University of Twente, The Netherlands

§Centre for Drug Research
University of Helsinki, Finland

¶School of Pharmacy
University of Otago, New Zealand

Coherent anti-Stokes Raman scattering (CARS) microscopy is used to visualize the release of a model drug (theophylline) from a lipid (tripalmitin) based tablet during dissolution. The effects of transformation and dissolution of the drug are imaged in real time. This study reveals that the manufacturing process causes significant differences in the release process: tablets prepared from powder show formation of theophylline monohydrate on the surface which prevents a controlled drug release, whereas solid lipid extrudates did not show formation of monohydrate. This visualization technique can aid future tablet design.

Keywords: Drug release; coherent anti-Stokes Raman scattering (CARS) microscopy.

1. Introduction

Dissolution of drugs from solid pharmaceutical tablets is a complex process that depends on several properties of the drug and tablet, such as the distribution of the drug in the tablet and the nature and flow of the dissolution medium. One important factor that influences drug dissolution is the solid state form of the drug. During dissolution, the drug can transform to a less dissolvable hydrate.[1] For this reason, it is crucial that the solid-state properties are monitored during dissolution.

Coherent anti-Stokes Raman scattering (CARS) microscopy has been shown to be a chemically selective method for investigating highly

scattering media[2] using the Raman active vibrational modes with real-time[3] imaging. Hence, we expect that it is a suitable method for probing physicochemical phenomena in tablets, in which the drug is usually dispersed in particulate form, with such dosage forms constituting the majority of medicines currently marketed. The CARS is a four-photon non-linear process, where a pump photon of frequency ω_p, a Stokes photon of frequency ω_s and probe photon of frequency ω'_p (taken the same as the pump frequency) interact with the sample and generate an anti-Stokes photon of frequency $\omega_{as} = \omega_p - \omega_s + \omega'_p$. The CARS signal is resonantly enhanced when the difference frequency $\omega_p - \omega_s$ coincides with a molecular vibrational level transition. With CARS, it is possible to achieve temporally and spatially resolved visualization[4,5] of the distribution and the solid-state properties of the powders and tablets. This study focuses on the visualization of drug dissolution and solid-state transformations.

2. Experimental System

The CARS set-up is based on a Coherent Paladin Nd:YAG laser and an APE Levante Emerald optical parametric oscillator (OPO). The fundamental (1064 nm) of the laser is used as Stokes, whereas the signal from the OPO (tunable between 700 nm and 1000 nm) is used as the pump and probe. The beams are scanned over the sample by galvano mirrors (Olympus FluoView 300, IX71) and focused by a 20×0.5 NA objective lens into the sample. Both beams have a power of several tens of mW at the sample. Due to the highly scattering samples, the forward-generated CARS signal is collected in the backward direction.[2] The collected signal is filtered and detected by a photo multiplier tube. All images are 512×512 pixels and obtained in 2 seconds.

To determine suitable vibrational bands for component-specific imaging and analysis, Raman spectra were recorded of pure tripalmitin, theophylline anhydrate, and monohydrate and water with a 1600 pixels CCD camera (Newton DU-970N, Andor Technology) (Fig. 1). The samples were irradiated by a Kr ion Laser (Coherent, Innova 90K) at 647.1 nm of 30 mW and focused by 40×0.65 NA microscope objective lens. Care was taken to ensure that the focal spot was filled with pure material. The spectra are shown in Fig. 2. Figure 2(a) shows the spectra of the three powdered substances. The region exhibiting the large spectral

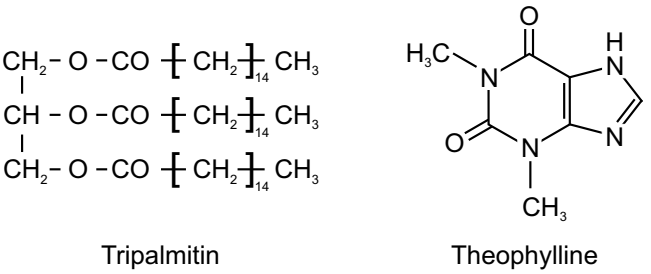

Fig. 1. Molecular structure formula of the lipid tripalmitin and drug theophylline.

differences between the components is highlighted in gray and also featured in Fig. 2(b). Between 2700 cm^{-1} and 3200 cm^{-1}, the CH stretch in the aldehyde function of tripalmitin gives rise to a peak at 2715 cm^{-1} whereas the CH_2 and CH_3 symmetric stretching in the fatty acid chains correspond to peaks at 2850 cm^{-1} and 2880 cm^{-1}, respectively.[6] Theophylline exhibits CH stretching at 3109 cm^{-1} for the theophylline monohydrate and 3123 cm^{-1} anhydrate.[7,8] Specific component analysis in the 1600–1800 cm^{-1} region is not favorable due to the water vibrational modes around 1650 cm^{-1} and cannot be used for real-time dissolution experiments. In the 2700–3200 cm^{-1} region, tripalmitin and theophylline can be imaged selectively using peaks at 2880 cm^{-1} (tripalmitin) and 3109 cm^{-1} (theophylline). Unfortunately, a distinction between theophylline anhydrate and monohydrate is not possible in this region. Nevertheless, the peak at 3109 cm^{-1} can be used to image selectively both forms of theophylline. The interference from water in this region would seem large as well, but these bands are so broad and de-phase so quickly that their influence is limited.

For a qualitative and quantitative monitoring of the drug distribution in the tablet during dissolution, a translation has to be made from the Raman spectra to the CARS images. Using the images at 2880 cm^{-1} and 3109 cm^{-1}, the concentration of theophylline can be related to the concentration of the tripalmitin. Since the tripalmitin stays intact during dissolution, it can serve as the marker for the local theophylline concentration, which is known from the fabrication. The Raman spectra are related to the CARS spectra, but they are not the same. In short, Raman spectra depend linearly on the constituent concentration whereas the CARS spectra depend quadratically on concentration. The Raman spectral intensity can be expressed as the imaginary part of the (resonant) CARS amplitude.[9]

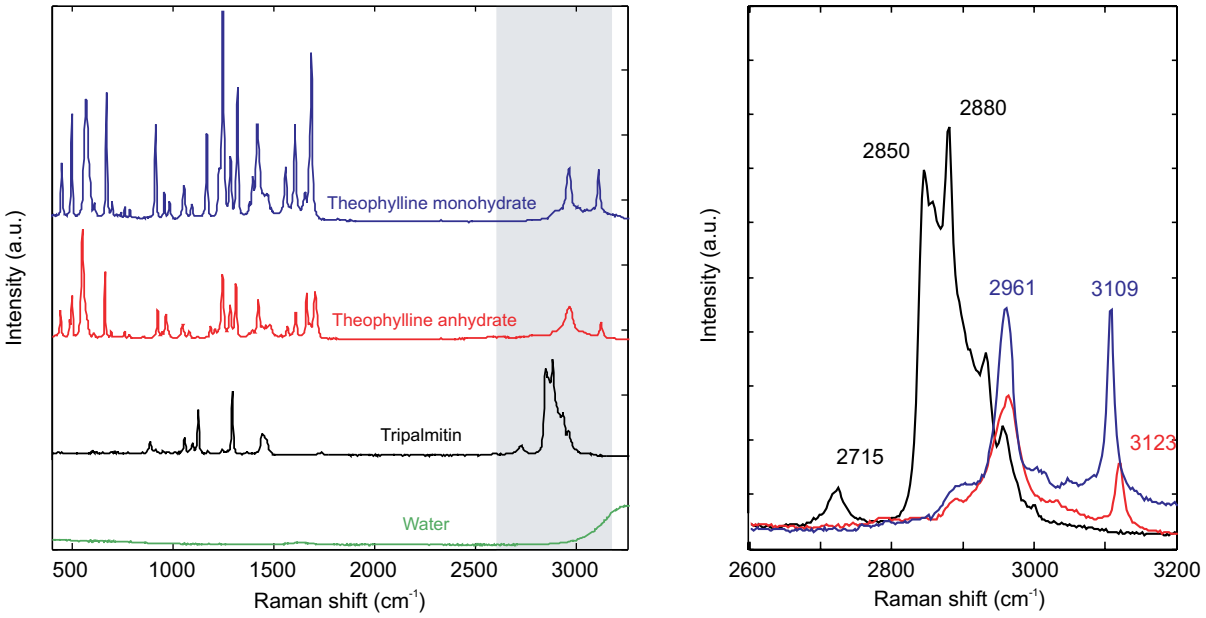

(a) (b)

Fig. 2. Raman spectra of the powdered substances and water: (a) full spectra of tripalmitin (black), theophylline anhydrate (red), theophylline monohydrate (blue), and water (green) and (b) highlighted detail of image (a).

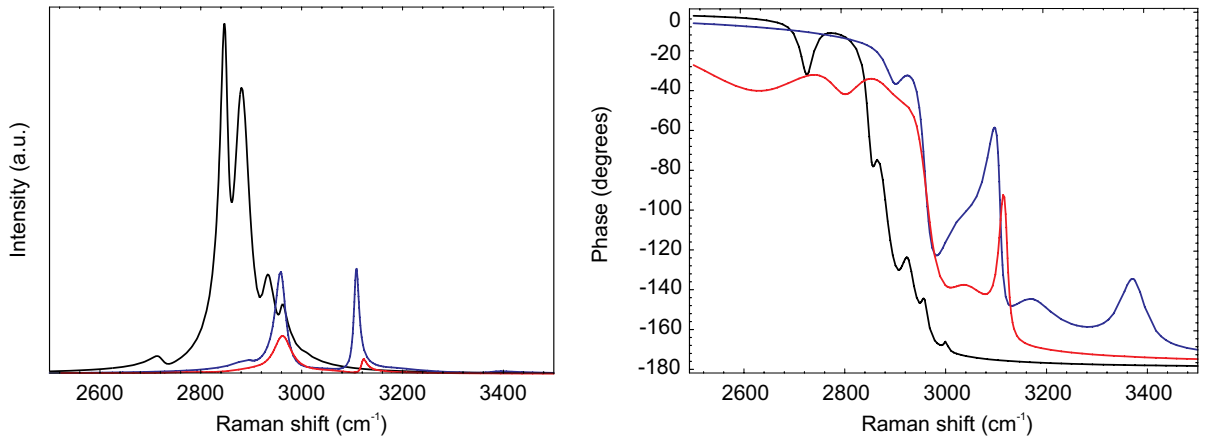

(a) (b)

Fig. 3. Simulation on Raman data (Fig. 2) of tripalmitin (black), theophylline anhydrate (red), theophylline monohydrate (blue), to obtain the (a) resonant CARS spectra and (b) CARS phase.

To simulate the CARS spectra, the Raman data were fitted to the imaginary part of multiple complex Lorentzians. The resonant part of the CARS intensity spectra and their phases are depicted in Fig. 3. The full CARS spectra also contain a non-resonant part that cannot be deduced from the Raman measurement. This real part can be effectively described as a constant where the magnitude depends on the excitation pulse lengths and wavelengths. For our experiments, the non-resonant component can be estimated as somewhere between 1% and 10% of the peak resonant amplitude. This non-resonant contribution has little effect on the signal intensity close to a resonance.

The CARS spectra shown in Fig. 3 reveal that the different powders have partially overlapping spectra. To overlay and compare the CARS images obtained at different vibrational resonances, weight factors have to be found based on the CARS spectra. Around 2880 cm^{-1}, the CARS intensity

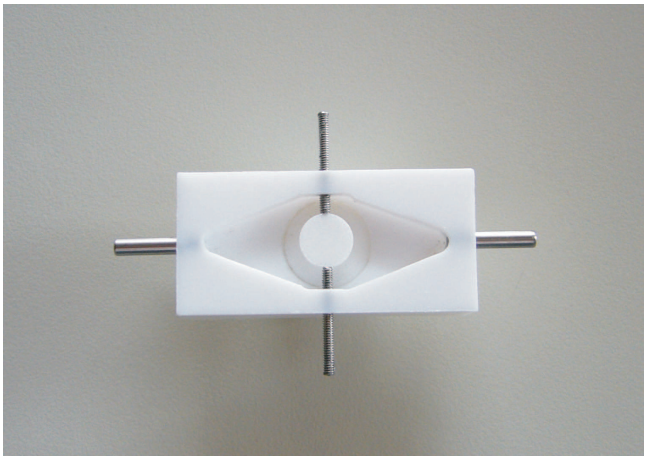

Fig. 4. Photograph of the flow cell with tablet (without the cover glass).

for tripalmitin exceeds the intensity for the theophylline (both monohydrate and anhydrate) by a factor of 20. The images obtained at $2880\,\mathrm{cm}^{-1}$ can thus be taken to represent the tripalmitin density distribution (absolute squared). At $3109\,\mathrm{cm}^{-1}$, the CARS intensity for the monohydrate exceeds the tripalmitin by a factor of 18. The intensity for the monohydrate is closer to the tripalmitin so that the precise ratio is strongly influenced by the amount of non-resonant background. From the images, it is clear that the monohydrate exceeds the tripalmitin by a factor larger than 3, based on areas that could be identified to contain only one of the constituents.

The images at different wavelengths can be related to each other by picking a spot containing pure tripalmitin and scaling the intensity in the $3109\,\mathrm{cm}^{-1}$ image to reflect the correct ratio. Furthermore, the phase of the tripalmitin signal is between 70 and 90 degrees separated from the signal of the theophylline (monohydrate or anhydrate). Therefore, the total signal from a combination of the powders, which is given by the absolute square of the combined amplitude, is almost equal to the addition of the absolute square of the components as is displayed in both images. The tripalmitin image, once correctly scaled, can thus be subtracted from the other image to obtain an almost pure image and this procedure is allowed even for regions that contain signals from both substances. Since the (initial) distribution of substances (Figs. 5(a), (d) and (g)) is coarse on the scale of the images, most pixels can be assigned to contain either tripalmitin or theophylline and the percentage of drug and lipid at the surface can be extracted simply by counting pixels which yields the coverage percentages mentioned in Fig. 5.

For a more precise analysis, the CARS amplitude and phase can be detected locally using heterodyne detection[10] to extract the relative components. This paper focuses on the qualitative description, further work will include detailed quantitative measurements.

In this study of dissolution from two different types of pharmaceutical tablets, three model systems of a drug (theophylline) in a matrix (tripalmitin) were investigated: (1) tablets of tripalmitin with theophylline *monohydrate*, created by tabletting a powder mixture, (2) tablets of tripalmitin with theophylline *anhydrate*, also from a powder mixture, and (3) tablets from an *extrudate* of tripalmitin with theophylline anhydrate. The details of the sample preparation are given elsewhere.[11] Two different types of experiments are performed: dissolution by immersion in purified water and dissolution by flowing purified water in a flow cell. The flow cell used for the *in situ* dissolution imaging consisted of a Teflon chamber with two metal bars that fix the tablets in the middle of a flowing water bed (Fig. 4). Purified water was constantly pumped through the cell. The lower side of the cell consists of a thin microscope cover glass that is placed on the microscope stage. This specific set-up allows *in situ* visualization of the solid-state properties of the tablets under pharmaceutically relevant dissolution conditions.

3. Results and Discussion

Figure 5 depicts false-color images of the surface of the three model systems. The drug is always depicted in green, irrespective of its solid-state form. The lipid matrix is depicted in red. The first column depicts the three dry systems. The surface of the theophylline monohydrate 5(a) is characterized by thin needles whereas the anhydrate 5(d) shows anisometric particles. The tablet of compressed extrudates 5(g) shows a smaller proportion of drug signal on the surface, so that the drug can be considered more embedded in the matrix (not observed on an uncompressed extrudate). On the dry tablet, the surface coverage was determined as: 5(a) tablet tripalmitin/theophylline monohydrate (40%/60%), 5(d) tablet tripalmitin/theophylline anhydrate (60%/40%) and 5(g) tablet of extrudates tripalmitin/theophylline anhydrate (20%/80%).

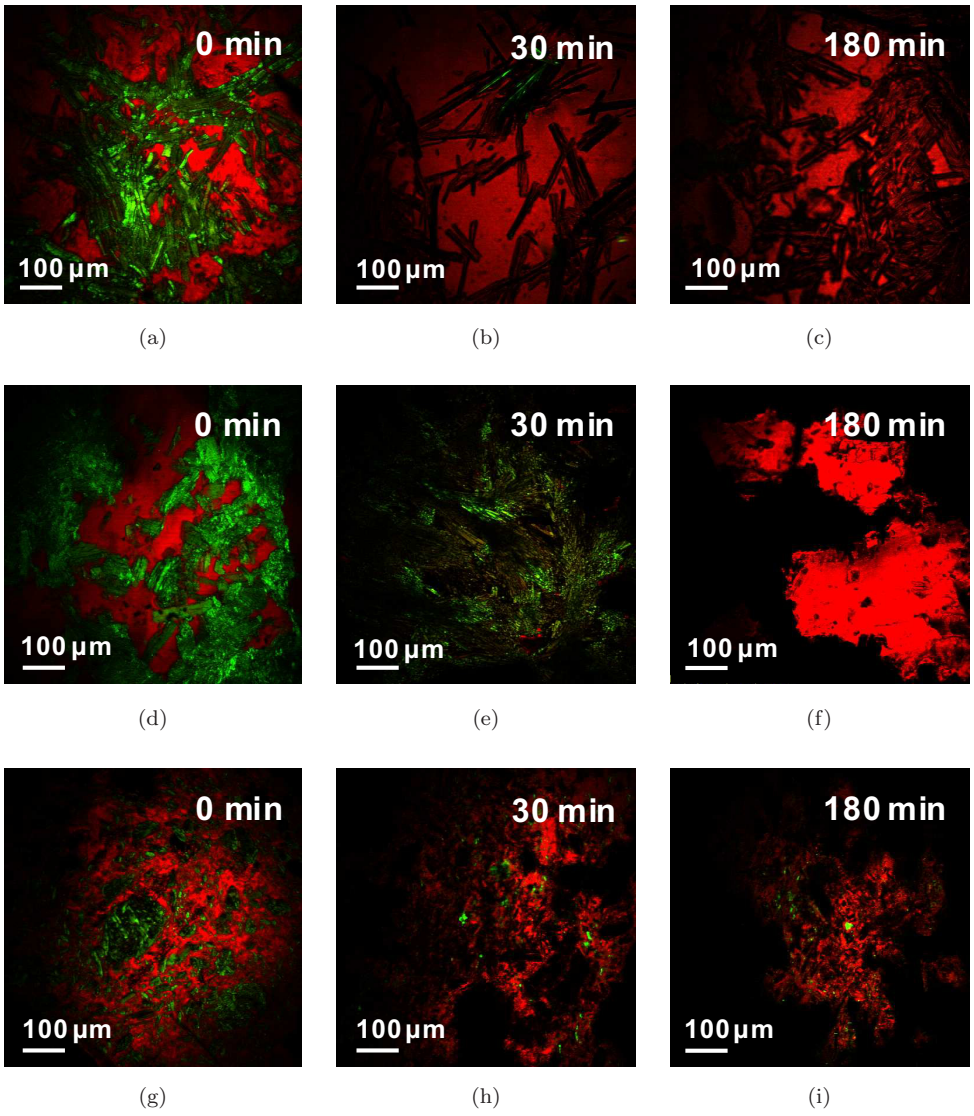

Fig. 5. Images of the lipid tripalmitin (2880 cm^{-1}, red) and drug theophylline (3109 cm^{-1}, green) after different durations of immersion. (a)–(c) tablet tripalmitin/theophylline monohydrate (d)–(f) tablet tripamitin/theophylline anhydrate (g)–(i) tablet of extrudates tripalmitin/theophylline anhydrate.

The release of drug and changes to the surface were first monitored by imaging after different immersion times. The tablets were immersed in 500 mL of purified water, and after defined time intervals, removed and imaged (Fig. 5). The tablet consisting of tripalmitin and theophylline monohydrate (Fig. 5(a) to (c)) shows the release of the drug from the matrix without significant surface alteration. The lipid matrix stays intact, while the drug dissolves within the matrix and then diffuses through the pores in the matrix. After 30 minutes, a few monohydrate needles are left, while after 180 minutes, no drug is evident on the surface of the tablet. Pores (dark) can be observed where drug needles were located. The tablet consisting of tripalmitin and theophylline anhydrate (Fig. 5(d) to (f)) shows significant surface effects. After 30 minutes, the surface of the tablet is covered with fine needles (Fig. 5(e)), which are most likely theophylline monohydrate that has a much lower solubility and crystallizes on the surface after transformation from the anhydrate form.[12–14] After 180 minutes of immersion in water, the needles have completely dissolved.

For the tablet of compressed extrudate (Fig. 5(g) to (i)), release of the anhydrate particles was observed *without* monohydrate needle formation. Additional tests were conducted using the uncompressed extrudates, where the absence

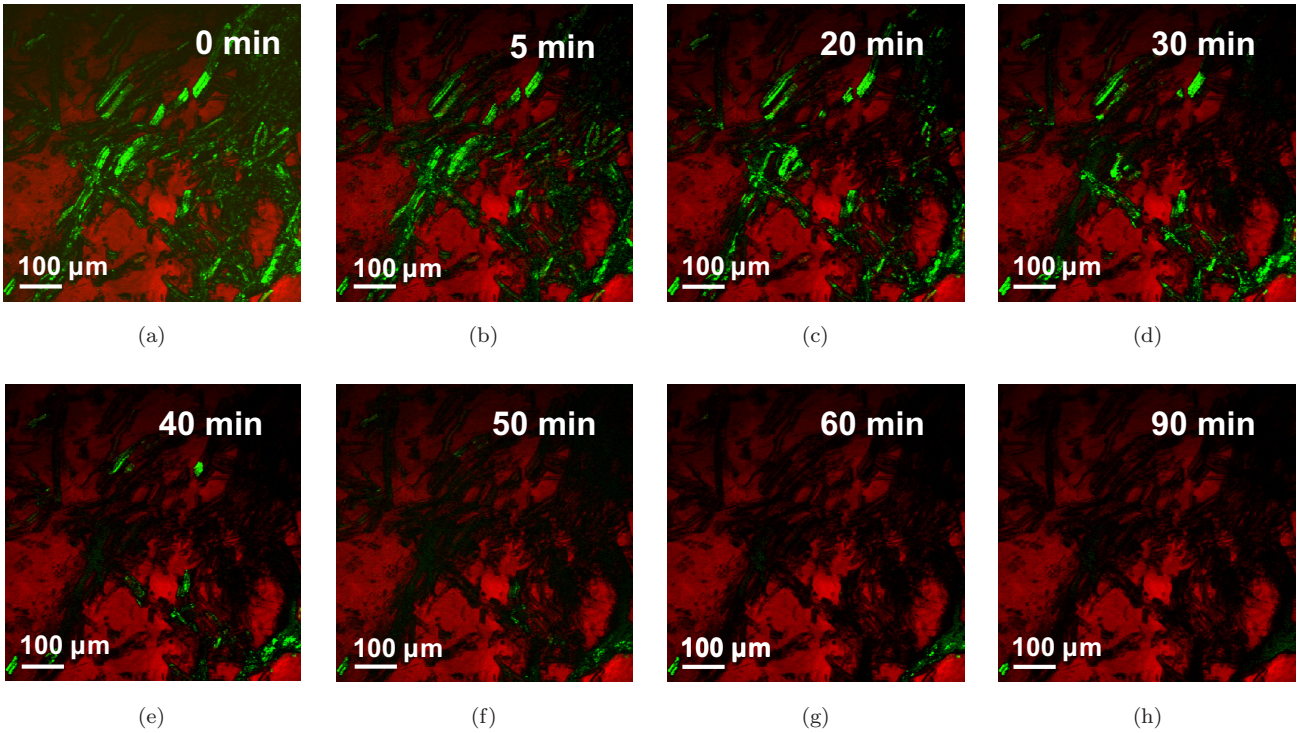

Fig. 6. *In situ* CARS imaging of drug release during dissolution in the flow cell. The lipid tripalmitin (2880 cm^{-1}, red) and drug theophylline monohydrate (3109 cm^{-1}, green).

of needle formation was confirmed. The smoother surface structure of the extrudate appears to prevent monohydrate crystallization. The solid-state transformations and crystal growth on a tablet containing pure theophylline anhydrate was also monitored *in situ*,[15] by placing the tablets in a vessel filled with water directly on the microscope stage. A thin stagnant water layer between the sample and the microscope cover slide promoted the growth of long needles which can be attributed to theophylline monohydrate formation.

For dissolution testing, tablets containing monohydrate were placed in the flow cell and continuously imaged over 90 minutes (Fig. 6). Focal drift and stability issues prevented a direct quantitative analysis of the images, but controlled release of the drug was clearly observed and quantitative analysis should be possible once the stability is improved.

4. Conclusion

CARS microscopy was combined with a pharmaceutically appropriate dissolution set-up and used to visualize the structure and distribution of a model drug in different tablets, as well as the changes during dissolution in real time. Such results provide valuable information about the physicochemical phenomena that may occur during drug dissolution. Theophylline anhydrate tends to form the monohydrate with a lower solubility during dissolution. The ability of the CARS set-up to distinguish between the different solid-state forms was investigated. Tablets made of lipid-based extrudates did not exhibit theophylline hydrate formation during drug dissolution. The difference between the two dosage forms is probably due to surface differences of the lipid matrix. Based on these results, CARS appears to be well-suited to the imaging of physicochemical changes in oral solid dosage forms during dissolution.

Acknowledgments

This research is supported by NanoNed, a nanotechnology program of the Dutch Ministry of Economic Affairs and partly financed by the Stichting voor Fundamenteel Onderzoek der Materie (FOM), which is financially supported by the Nederlandse Organisatie voor Wetenschappelijk Onderzoek (NWO). The Marie Curie Fellowship and the Galenos Network are acknowledged

for financial support (MEST-CT-2004-404992). The Sasol GmbH is acknowledged for generous provision of the lipids. We also acknowledge Coherent Inc. for the use of the Paladin laser and APE Berlin for the collaboration and use of a Levante Emerald OPO. Last but not least, we would like to acknowledge Chris Lee for bringing this collaboration possibility to our attention.

References

1. Brittain, H. G., *Polymorphism in Pharmaceutical Solids* (Marcel Dekker Inc., New York, 1999), pp. 279–330.
2. Cheng, J. X., Volkmer, A. and Xie, X. S., "Theoretical and experimental characterization of coherent anti-Stokes Raman scattering microscopy," *J. Opt. Soc. Am. B* 19, 1363–1375 (2002).
3. Evans, C. L., Potma, E. O., Puoris'haag, M., Cote, D., Lin, C. P. and Xie, X. S., "Chemical imaging of tissue *in vivo* with video-rate coherent anti-Stokes Raman scattering microscopy," *Proc. Natl. Acad. Sci. USA* **102**, 16807–16812 (2005).
4. Kang, E., Wang, H., Keun Kwon, I., Robinson, J., Park, K. and Cheng, J. X., "In situ visualization of Paclitaxel distribution and release by coherent anti-Stokes Raman scattering microscopy," *Anal. Chem.* **78**, 8036–8043 (2006).
5. Wang, H., Bao, N., Le, T. L., Lu, C. and Cheng, J. X., "Microfluidic CARS cytometry," *Opt. Express* **16**, 5782–5789 (2008).
6. De Smidt, J. H., Fokkens, J. G., Grjseels, H. and Crommelin, J. A., "Dissolution of theophylline monohydrate and anhydrous theophylline in buffer solutions," *J. Pharm. Sci.* **75**, 497–501 (1986).
7. Nolasco, M. M., Amado, A. M. and Ribeiro-Claro, P. J. A., "Computationally-assisted approach to the vibrational spectra of molecular crystals: Study of hydrogen-bonding and pseudo polymorphism," *Chem. Phys. Chem.* **7**, 2150–2161 (2006).
8. Amado, A. M., Nolasco, M. M. and Ribeiro-Claro, P. J. A., "Effect of moisture on crystallization of theophylline in tablets," *J. Pharm. Sci.* **96**, 1366–1379 (2007).
9. Potma, E. O., Evans, C. L., Xie, X. S., "Heterodyne coherent anti-Stokes Raman scattering (CARS) imaging," *Opt. Lett.* **31**, 241–243 (2006).
10. Jurna, M., Korterik, J. P., Otto, C. and Offerhaus, H. L., "Shot noise limited heterodyne detection of CARS signals," *Opt. Express* **15**(23), 15207–15213 (2007).
11. Windbergs, M., Strachan, C. J. and Kleinebudde, P., "Understanding the solid-state behaviour of triglyceride solid lipid extrudates and its influence on dissolution," to appear in *Eur. J. Pharm. Biopharm.*, available online June 2008.
12. Aaltonen, J., Heinäen, P., Peltonen, L., Kortejärvi, H., Tanninen, V. P., Christiansen, L., Hirvonen, J., Yliruusi, J. and Rantanen, J., "In-situ measurement of solvent-mediated phase transformations during dissolution testing," *J. Pharm. Sci.* **95**(12), 2730–2737 (2006).
13. Debnath, S., Predecki, P. and Suryanarayanan, R., "Use of glancing angle X-ray powder diffractometry to depth-profile phase transformations during dissolution of indomethacin and theophylline tablets," *Pharm. Res.* **21**, 149–159 (2004).
14. Ando, H., Ishii, M., Kayano, M. and Ozawa, H., "Effect of moisture in crystallization of theophylline in tablets," *Drug. Dev. Ind. Pharm.* **18**, 453–467 (1993).
15. Windbergs, M., Jurna, M., Herek, J. L., Offerhaus, H. L., Kleinebudde, P. and Strachan, C. J., "Visualization of the physicochemical structure of oral solid dosage forms and changes upon dissolution using coherent anti-Stokes Raman scattering microscopy," submitted to *Anal. Chem.*